

Novel Dissection Analysis of Spin-Orbit Coupling in the Type-B Cyclohexenone Photorearrangement. What Controls Photoreactivity? Mechanistic and Exploratory Organic Photochemistry^{1,2}

Howard E. Zimmerman* and Andrei G. Kutateladze

Department of Chemistry, University of Wisconsin, Madison, Wisconsin 53706

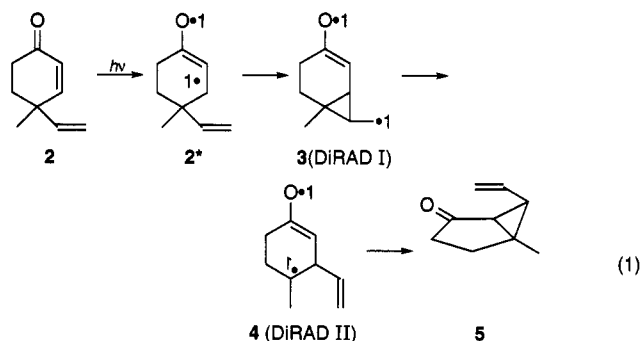
Received May 31, 1995 (Revised Manuscript Received August 10, 1995)

Two main concepts have been invoked as controlling the course of organic photochemical reactions. One is the nature of the excited state hypersurface with reacting molecules following minimum energy pathways toward geometries of alternative photoproducts.^{3a–c} The other is competitive excited state radiationless decay to the alternative ground state products,^{4a–e} by internal conversion of singlets or intersystem crossing of triplets. That such decay must occur is a truism; however, in our view decay controls the direction of excited state reactivity only for those simpler reactions where minimal geometric change occurs. More generally, when decay is a factor in a complex reaction it is far removed along the hypersurface.

In this paper we support this view and present important results in dealing with spin-orbit coupling⁵ control of intersystem crossing. The example of the type-B rearrangement of 4-arylcyclohexenones to afford 6-arylbicyclo[3.1.0]hexanones⁶ is used. We report: (a) Ab initio spin-orbit coupling dissection at strategic points along the type-B reaction hypersurface. (b) Spin-orbit coupling is dominated by geminal interactions. (c) Evidence that HOMO–LUMO considerations lead to errors and a larger active space is required. (d) Energetics along the hypersurfaces leading from reactant to product. (e) The largest contributors to spin-orbit coupling for reactant and product ketones are oxygen p_y – p_x (i.e., n – π^* type). But, for the diradical intermediates, spin-orbit coupling is dominated by geminal hybrid interactions at the odd-electron centers. (f) The relatively low experimental quantum yields are due to intersystem crossing from the enone reactant triplet to ground state rather than along the reaction hypersurface. (g) Final product formation results from T_1 to S_0 intersystem crossing in the region past “diradical II” as the bicyclic structure is

approached. (h) Evidence that for complex photochemical rearrangements, the reaction course is dictated by events on the excited state surface distant from the vertical excited state and controlled by the nature of the surface.

Computations were run for the 4,4-diphenylcyclohexenone (**1**)⁶ and 4-methyl-4-vinylcyclohexenone (**2**)⁷ sys-



tems of reactant enone, diradical I, diradical II, and bicyclic photoproduct. Note eqs 1 and 2. For computational simplicity, a more complete study was carried out using the vinylenone system where a more extended active space was possible.⁸ Ab initio energies, total spin-orbit coupling (SOC), and dissected SOC were obtained by methods we previously described.^{3a}

Use of the commonly employed HOMO–LUMO approximation leads to errors. Note Table 1. Reactant and product ketones require an increased active space to provide complete SOC contributions, although intermediate reacting diradicals provided more complete SOC values with lesser active spaces. This is seen particularly clearly in the case of bicyclic ketone **5** where only MO's below HOMO contained appreciable p_y (i.e., “ n ”) weighting. The role of n – π^* excitation in organic photochemistry has long literature precedent.^{3b,c,11}

Interestingly, the major contributions involve spin-orbit coupling *between geminal orbital pairs* with heavy weighting at the odd-electron centers. While anticipated for ketones with their oxygen “ n ” (i.e., p_y) and the p – π orbitals, past literature discussions have emphasized interactions *between odd-electron centers*. Interactions between orbitals at two different centers proved much smaller. Note Table 2 for the largest SOC contributions in the triplet species of interest. For example, in Table 2, the interaction between orbitals p_3 and p_5 is seen to be small.

We were also interested in the energetics of the type-B enone rearrangement. Figure 2 shows ab initio energies obtained at critical points along the hypersurface for the vinylenone **2**, namely the T_1 energies of enone **2**, diradical

(1) This is publication 175 of our photochemical series and 238 of the general sequence.

(2) Part 174: Zimmerman, H. E.; Zhu, Zhaoning *J. Am. Chem. Soc.* **1995**, *117*, 5245–5262.

(3) (a) Zimmerman, H. E.; Kutateladze, A. G.; Maekawa, Y.; Mangette, J. E. *J. Am. Chem. Soc.* **1994**, *116*, 9795–9796. (b) Zimmerman, H. E. 17th National Organic Symposium of the American Chemical Society, Bloomington, IN, 1961; pp 31–41. (c) Zimmerman, H. E.; Schuster, D. I. *J. Am. Chem. Soc.* **1962**, *84*, 4527–4540.

(4) (a) Zimmerman, H. E. *J. Am. Chem. Soc.* **1966**, *88*, 1566–1567. (b) Zimmerman, H. E. *Acc. Chem. Res.* **1972**, *5*, 393–401. (c) Michl, *J. Mol. Photochem.* **1972**, 243–255, 257–286, 287–314. (d) Zimmerman, H. E.; Factor, R. E. *J. Am. Chem. Soc.* **1980**, *102*, 3538–3548. (e) Requero, M.; Olivucci, M.; Bernardi, F.; Robb, M. A. *J. Am. Chem. Soc.* **1994**, *116*, 2103–2114 and related papers cited therein.

(5) Spin-orbit coupling is most important in singlet–triplet interconversion.

(6) (a) Zimmerman, H. E.; Cowley, B. R.; Tseng, C.-Y.; Wilson, J. W. *J. Am. Chem. Soc.* **1964**, *86*, 947–948. (b) Computations on the diphenylcyclohexenone system proved parallel to the simple vinyl enone **2**. The active space possible for the diphenyl system was limited to (6,6), which was sufficient for the two diradicals. Again, the large contributions were geminal.

(7) (a) The triplet type-B rearrangement of 4-phenyl-4-vinylcyclohexenone has been reported by Swenton,^{7b} and the corresponding reaction of 4-methyl-4-propenylcyclohexenone is known from the research of Schaffner.^{7c} (b) Swenton, J. S.; Blankenship, R. M.; Sanitra, R. J. *J. Am. Chem. Soc.* **1975**, *97*, 4941–4947. (c) Nobs, R.; Burger, U.; Schaffner, K. *Helv. Chim. Acta* **1977**, *60* 1607–1628.

(8) AM1 was used for initial geometry optimization, GAMESS⁹ was employed for C.I. and total SOC. WISC SOC^{3a} dissects overall spin-orbit coupling into two-basis orbital components, with Weinhold natural hybrid orbitals (NHO)¹⁰ being the choice basis. This required SOC integrals in an NHO basis. AO SOC integrals available in GAMESS were transformed to the NHO basis. An STO-3G basis set was used in order to avoid the ambiguity of adding 2p and 3p components.

(9) Schmidt, M. W. et al. *J. Comput. Chem.* **1993**, *14*, 1347–1363.

(10) Reed, A. E.; Curtiss, L. A.; Weinhold, F. *Chem. Rev.* **1988**, *88*, 899–926.

(11) Kasha, M. In *Light and Life*; McElroy, W. D., Glass, B., Eds.; Johns Hopkins Press: Baltimore, 1961; p 31.

Table 1. Spin Orbit Coupling of Relevant Triplet Species in Eq 2 (cm⁻¹)

active space ^a	vinyl enone 2	diradical I	diradical II	closing species ^b		[3.1.0] vinyl bicyclic
				endo	exo	
2,2	0.0931	0.129	0.080	2.91	3.02	0.24
4,4	0.0148	0.313	0.122	2.94	2.92	1.12
6,6	0.0138	0.217	0.120	2.93	2.89	66.00
8,8	80.404	0.202	0.100	2.73	2.72	72.94
10,10	80.342			2.78		74.24

^a Number of active MOs and electrons. ^b Diradical II closing bond 3–5 fixed at 2.14 Å (note Figure 1 for orbital numbering) with geometry optimization.

Table 2. Selected NHO's RMS SOC Contributions for Species in Eq 2 (cm⁻¹)

enone		diradical I		diradical II	
hybrid pair	local SOC	hybrid pair	local SOC	hybrid pair	local SOC
n _{1y} -π ₁₂	80.906	p ₉ -σ ₉₈	0.173	n _{1y} -π ₁₂	0.142
n _{1y} -σ ₁₂	10.071	n _{1y} -π ₁₂	0.139	p ₅ -σ ₅₄	0.115
n _{1y} -π ₂₁	2.322	p ₃ -σ ₃₄	0.072	p ₈ -σ ₃₄	0.094
				p ₃ -p ₅	0.005

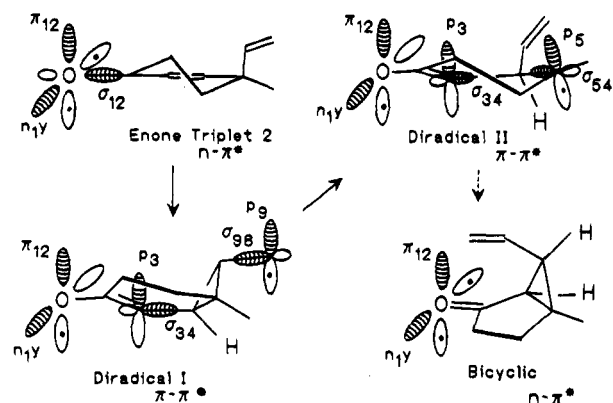
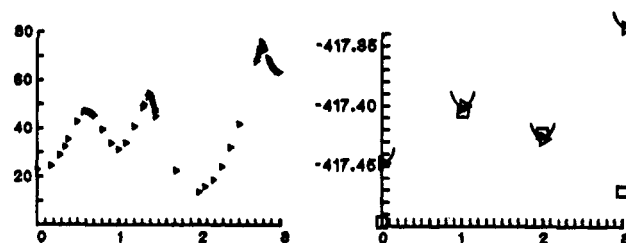
endo closing species		exo closing species		bicyclic	
hybrid pair	local SOC	hybrid pair	local SOC	hybrid pair	local SOC
p ₅ -σ ₅₄	1.970	p ₅ -σ ₅₄	2.073	n _{1y} -π ₁₂	70.030
p ₃ -σ ₃₄	1.749	p ₃ -σ ₃₄	1.828	σ ₂₇ -π ₂₁	3.315
n _{1y} -π ₁₂	0.950	n _{1y} -π ₁₂	0.962	n _{1y} -π ₂₁	3.157
p ₃ -p ₅	0.479	p ₃ -p ₅	0.461	n _{1y} -σ ₁₂	2.782
				σ ₂₃ -π ₂₁	2.600

I 3, diradical II 4, and bicyclic triplet 5. In addition, for selected species of interest, corresponding vertical CASSCF S₀ energies were obtained using AM1¹² optimized triplet geometries. The enone triplet and diradicals I and II are minima on the reaction pathway. We note that an experimental 10.5 kcal/mol barrier for formation of diradical I from 4,4-diphenylcyclohexenone triplet has been reported.¹³

This energy barrier along with the observed large spin-orbit coupling in the n-π* enone triplet accounts for the relatively low quantum yields^{13,14} in type B enone rearrangements leading to enone radiationless triplet decay. Very small spin-orbit coupling was found for diradicals I and II which follow on the triplet hypersurface. On the hypersurface, the triplet changes from n-π* to π-π* and back to n-π*; note Figure 1.

The point of decay seems to be near "closing species" 6 (Table 1) which is between diradical II and bicyclic product. SOC is increasing and intersystem crossing to S₀ product occurs before the energy increase becomes too large.

Interestingly, the increase in spin-orbit coupling in the "closing species" 6 does not arise from direct 3,5-orbital interaction as might be thought. Although the local dissection reveals carbons 3 and 5 to play a dominant role, the major contributions are geminal at these centers. The dependence of spin-orbit coupling on the relative

**Figure 1.** Vinyl enone 2, diradical intermediates, and bicyclic 8.**Figure 2.** (a, top) AM1 energies, kcal/mol. (b, bottom) ab initio energies, hartrees. Both plotted against a reaction coordinate with abscissa points labeled as 0, 1, 2, and 3 as follows: 0, enone reactant; 1, diradical I; 2, diradical II; 3, bicyclic product. Triangles indicate T₁; squares indicate S₀.

orientation of orbitals at two diradical centers arises not from their direct interaction but rather from the wavefunction for each MO which relates the orientation of an orbital at one center to the other.

Most important, it is seen that the course of such a complex photochemical rearrangement is controlled by hypersurface characteristics not necessarily near the reactant vertical excited state but far removed from this geometry. The two most important features controlling excited reactivity are (a) excited state energy barriers and (b) the probability of conversion of excited state to ground state. For triplets, intersystem crossing to the ground state surface is aided by spin-orbit coupling. Singlets require a counterpart internal conversion via conical intersections.^{14,3b} However, the factors aiding decay to ground state alone seem insufficient for reaction. Such decay near reactant geometry generally diminishes efficiency while decay with geometry near product geometry enhances reactivity. This is close to our much earlier postulate that photochemical reactivity is governed by the tendency of molecules to seek out energy valleys and mountain passes on the excited state surface.^{3b,c} Hence, often excited state chemistry is reminiscent of ground state reactivity.

Acknowledgment. Support of this research by the National Science Foundation is gratefully acknowledged.

Supporting Information Available: Computational methodology and detailed results (81 pages).

JO950980J

(12) Dewar, M. J. S.; Zoebisch, E. G.; Healy, E. F.; Stewart, J. J. P. *J. Am. Chem. Soc.* **1985**, *107*, 3902–3909 (MOPAC Ver. 6.0).

(13) Zimmerman, H. E.; Elser, W. R. *J. Am. Chem. Soc.* **1969**, *91*, 887–896.

(14) Zimmerman, H. E.; Hancock, K. G. *J. Am. Chem. Soc.* **1968**, *90*, 3749–3760.